

Synthesis, NLO and Theoretical modeling of the Anti-inflammatory potential of six DibenzylideneCyclopentanone analogues of Curcumin

By

**Chelli Sai Manohar, N. Sai Pavan Chakravarthy,
G. Nageswara Rao and B. Siva Kumar**

ISSN 2319-3077 Online/Electronic

ISSN 0970-4973 Print

UGC Approved Journal No. 62923

MCI Validated Journal

Index Copernicus International Value

IC Value of Journal 82.43 Poland, Europe (2016)

Journal Impact Factor: 4.275

Global Impact factor of Journal: 0.876

Scientific Journals Impact Factor: 3.285

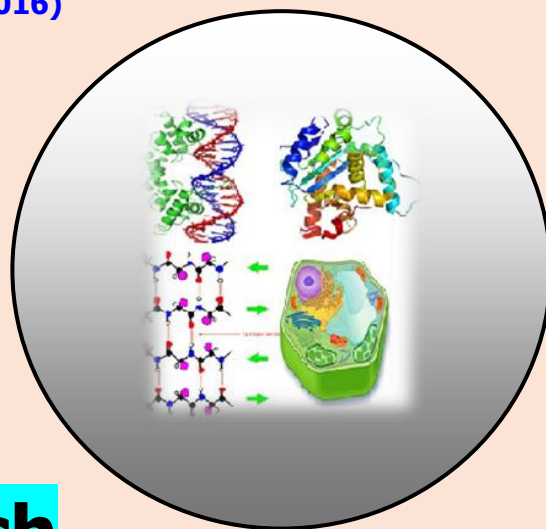
InfoBase Impact Factor: 3.66

J. Biol. Chem. Research

Volume 35 (2) 2018 Pages No. 996-1008

Journal of Biological and Chemical Research

An International Peer Reviewed / Referred Journal of Life Sciences and Chemistry



**Indexed, Abstracted and Cited in various International and
National Scientific Databases**

Published by Society for Advancement of Sciences®

J. Biol. Chem. Research. Vol. 35, No. 2: 996-1008, 2018

(An International Peer Reviewed / Refereed Journal of Life Sciences and Chemistry)

Ms 36/01/31/2019

All rights reserved

ISSN 2319-3077 (Online/Electronic)**ISSN 0970-4973 (Print)**

Dr. B. Siva Kumar

[http:// www.sasjournals.com](http://www.sasjournals.com)[http:// www.jbcr.co.in](http://www.jbcr.co.in)jbicchemres@gmail.com

RESEARCH PAPER

Received: 18/10/2018

Revised: 13/12/2018

Accepted: 14/12/2018

Synthesis, NLO and Theoretical modeling of the Anti-inflammatory potential of six DibenzylideneCyclopentanone analogues of Curcumin

Chelli Sai Manohar, N. Sai Pavan Chakravarthy,
G. Nageswara Rao and B. Siva Kumar

Department of Chemistry, Sri Sathya Sai Institute of Higher Learning,
Vidyagiri Prasanthi Nilayam, Andhra Pradesh 515134, India

ABSTRACT

Cyclopentanone analogues specifically have been noted as potential leads for anti-inflammatory activity with promising nonlinear optical properties. Six novel cyclopentanone analogs were synthesized and extensively characterized using Fourier Transform-Infrared spectroscopy (FT-IR), UV-Vis spectroscopy, NMR and Mass spectrometry, and their NonLinear Optical (NLO) properties were evaluated. A 'theoretical' study via ab initio DFT simulations was undertaken that demonstrated the significant correlation to the experimental findings with respect to both structural conformation and IR vibrational modes. In conclusion, the in silico anti-inflammatory activity was explored to predict their drug potential as anti-inflammatory agents via the molecular docking studies of analogous cyclopentanone derivatives, pursuing the mechanism of Mammalian Thioredoxin reductase. The corresponding qualitative structure activity relationship was also elucidated.

Keywords: DBA, DFT, Nonlinear Optics, Molecular Docking, Anti-inflammatory agents

INTRODUCTION

Hetero-aryl derivatives of DBA are popular curcumin analogs owing to their stability and wide range of medicinal activity, especially in appreciable anti-malarial and anti-bacterial activity (Bukhari et al. 2013; Anand et al. 2007). Cyclopentanone analogues are monocarbonyl analogues of curcumin synthesized by the Claisen-Schmidt condensation reaction between cyclopentanone and an aldehyde. They demonstrated modest anti-cancer potential (Liang, Shao, et al. 2009) with almost 51 times the potency of curcumin in bone cancer treatment (Leow et al. 2014). They have also exhibited potent anti-oxidant activity with respect to the Keap-1/Nrf2 pathway (Dinkova-Kostova and Talalay 2008), supported by theoretical studies evaluating the significant correlations (Chen et al. 2014; Shang et al. 2010). However, the major promise has been their anti-inflammatory activity with the corresponding extensive QSAR studies (Wang et al. 2012; Liang et al. 2008; Zhao et al. 2010; Liang, Yang, et al. 2009).

Computer aided drug design has become the widely popular approach to tackle the constraints of resources and tedious efforts into the whole process. There have been tremendous theoretical success in establishing the mechanism of photosensitivity in curcumin probed with TD-DFT studies (Shen, Ji, and Zhang 2005; Shen and Ji 2007). These studies have also helped demonstrate the significant correlation to the experimental characterization (Benassi et al. 2008), and extensive DFT, vibrational and NBO analysis for 2,5-bis(4-hydroxy-3-

Indexed, Abstracted and Cited in Indexed Copernicus International and 20 other databases of National and International repute

methoxybenzylidene)-cyclopentanone(Saleem et al. 2011).We have therefore approached a similar theoretical support for our molecules. Those molecules with no studies reported thus far on their enzyme inhibition, DFT treatment or crystal structure were synthesized, characterized and tested for their SHG (Second-Harmonic Generation) properties(Corn and Higgins 1994).

Thus, the present study pursues the modeling of anti-inflammatory activity with the synthesized set of six novel cyclopentanone analogs. The two common pathways for the anti-inflammatory activity are noted to be the *Thioredoxin reductase* and *Aldose reductase* pathways. It was also found that there was no sufficient data regarding the QSAR equation of cyclopentanone analogues in these pathways. Given that cyclopentanone derivatives are potent inhibitors of both the enzymes(Liu et al. 2008; Du et al. 2006),and to help in the rapid screening of inhibitors, we pursued a correlation for the effect of the binding affinity on the desired biological activity that could be evaluated by a molecular docking study. We thus undertake an extensive experimental and theoretical treatment of cyclopentanone derivatives – ortho and meta chlorobenzylidene substitution, orthofurfurylideneand thienylmethylidenesubstitution, and ortho and para hydroxybenzylidenesubstitution - to evaluate their potential as anti-inflammatory leads.

MATERIALS AND METHODS

Synthesis of Cyclopentanone analogues

Synthesis of 2,5,-Bis(2-chlorobenzylidene)cyclopentanone

To a stirred solution of NaOH (6.25g) in 125 ml of water and ethanol (1:1), one half of a previously prepared mixture of 0.0615 moles (7.1ml) of 2-chlorobenzaldehyde and 0.03125 moles (2.8ml) of cyclopentanone was added and stirred. After 15 minutes, the remaining solution was added and the reaction was continued for 45 minutes. The precipitated product was then filtered and washed with cold water till the washings were free of base. The crude product was then recrystallized from methanol to get the pure product. (Yield – 88%, m.p.-153-155°C). The purity of the compound was ascertained by the single spot on TLC using a 4:1 pet ether-ethyl acetate system as the eluant(R_f Value – 0.64).

Synthesis of 2,5,-Bis(3-chlorobenzylidene)cyclopentanone

To a stirred solution of NaOH (6.25g) in 125 ml of water and ethanol (1:1), one half of a previously prepared mixture of 0.0615 mol (7.2ml) of 3-chlorobenzaldehyde and 0.03125 mol (2.8ml) of cyclopentanone was added and stirred. After 15 min, the remaining solution was added and the reaction was continued for 45 minutes. The precipitated product was then filtered and washed with cold water till the washings were free of base. The crude product was then recrystallized from methanol to get the pure product (Yield- 86%, m.p. -174-176°C). The purity of the compound was ascertained by the single spot on TLC using a 4.5:0.5 pet ether-ethyl acetate system as the eluant (R_f Value – 0.57).

Synthesis of 2,5,-Bis(2-furfurylidene)cyclopentanone

To a stirred solution of NaOH (6.25g) in 125 ml of water and ethanol (1:1), one half of a previously prepared mixture of 0.0615 moles (5.1ml) of 2-furfural and 0.03125 moles (2.8ml) of cyclopentanone was added with stirring. After 15 minutes, the remaining solution was added and the reaction was continued for 45 minutes. The precipitated product was then filtered and washed with cold water till the washings were free of base. The crude product was then recrystallized from methanol to get the pure product(Yield-79%, m.p. - 161-163°C). The purity of the compound was ascertained by the single spot on TLC using a 4:1 chloroform-methanol system as the eluant (R_f Value – 0.48).

Synthesis of 2,5-Bis((2-thienyl)methylidene)cyclopentanone

To a stirred solution of NaOH (6.25g) in 125 ml of water and ethanol (1:1), one half of a previously prepared mixture of 0.0615 moles (5.8ml) of 2-thiophenylaldehyde and 0.03125 moles of cyclopentanone (2.8 ml) was added with stirring. After 15 minutes, the remaining solution was added and the reaction was continued for 45 minutes. The precipitated product was then filtered and washed with cold water till the washings were free of base. The crude product was then recrystallized from ethanol to get the pure product(Yield-73%, m.p. -174-176°C). The purity of the compound was ascertained by the single spot on TLC using a 4:1 Pet Ether-Ethyl acetate system as the eluant (R_f Value – 0.70).

Synthesis of 2,5-Bis(2-hydroxybenzylidene)cyclopentanone

To 40 ml of an inert ethanol and water (1:1)solution, 7.5g of NaOH was added and stirred. To this, half of a previously made mixture of 0.0625 moles (6.1ml) of salicylaldehyde and 0.0325 moles (2.9 ml) of cyclopentanone was added and stirred for 30 minutes.

The remainder of the mixture was then added and the reaction was allowed to continue for 4 hours. The solution was then cooled in ice and worked up with 50% solution of HCl, till the pH was lesser than 5. The precipitate formed was filtered and washed with cold water till the washings were free of acid. The substance was then dried and recrystallized from acetone to get the pure compound (Yield-75%, m.p. -195-197°C). The purity of the compound was ascertained by the single spot on TLC using a 4.5:0.5 chloroform-methanol system as the eluant (R_f Value – 0.70).

Synthesis of 2,5-bis(4-Hydroxybenzylidene) cyclopentanone

To a 1:1 mixture (40 ml) of ethanol and water, previously flushed with nitrogen, 7.5g of NaOH was added and stirred. To this, half of a previously made mixture of 0.0625 moles (6.1ml) of 4-hydroxybenzaldehyde and 0.0325 moles (7.63 g) of cyclopentanone was added and stirred for 30 minutes. The remainder of the mixture was then added and the reaction was allowed to continue for 4 hours. The solution was then cooled in ice and worked up using a 50% solution of HCl, till the pH was lesser than 5. The precipitate formed was filtered and washed with cold water till the washings were free of acid. The substance was then dried and recrystallized from acetone to get the pure compound (Yield-83%, mp -192-194°C). The purity of the compound was ascertained by getting a single spot on TLC using a 4.5:0.5 chloroform-methanol system as the eluant (R_f Value – 0.66).

The characterization of these derivatives undertaken to elucidate the structure recorded the follows:

2,5-bis(2-Chlorobenzylidene)cyclopentanone

Yellow crystalline solid; yield - 88%; mp: 153-156°C; IR (cm^{-1}) – 1687,1620,1600,1449, 1385,1038,988,751;¹H NMR (δ in ppm)- 3.02 (4H,s), 7.35 (4H,m), 7.45 (2H,d), 7.56 (2H,d), 7.94 (2H,s); ¹³C NMR (δ in ppm)– 26.6, 126.6, 130.0, 130.1, 130.2, 130.7,133.8,136.1,139.3,195.5; UV (λ_{max} in nm) -271,344; Mass (M/Z): (260.9,278.9,292.9,328.9 - [M+H] peak).

2,5-bis(3-Chlorobenzylidene)cyclopentanone

Yellow amorphous solid; yield- 86%; mp: 174-176°C; IR (cm^{-1})–1696, 1610,1600,1453, 1100,1083,991,886,791,673; ¹H NMR (δ in ppm)- 3.13 (4H,s), 7.35(4H,m), 7.45(2H,d), 7.56 (2H,s), 7.58 (2H,s);¹³C NMR (δ in ppm) – 26.4, 128.9, 129.4, 130.02, 130.1, 132.6, 134.7,137.4,138.2,195.9;UV (λ_{max} in nm) - 270,346; Mass (M/Z): (260.9, 278.9,292.9, 328.9 - [M+H] peak).

2,5-bis(2-Hydroxybenzylidene)cyclopentanone

Orange amorphous solid; yield-75%; mp: 195-197°C;IR (cm^{-1})– 3425,1630,1603, 1457, 1384,1351,988,745;¹H NMR (δ in ppm) - 2.83 (4H,s), 6.7 (2H,t), 6.9 (2H,d), 7.35 (2H,t),7.54 (2H,d),7.79 (2H,s), 10.14 (2H,s);¹³C NMR (δ in ppm)- 26.6, 116.1, 119.6, 122.9, 127.4, 130.6, 131.4,136.9,157.0,195.8; UV (λ_{max} in nm) - 270,343; Mass (M/Z): (187,275,293 - [M+H] peak).

2,5-bis((2-Thienyl)methylidene)cyclopentanone

Yellow amorphous solid; yield-73%;mp: 174-176°C;IR (cm^{-1})–1681,1593, 1365; ¹H NMR (δ in ppm) - 3.1 (4H,s), 7.1 (2H,t), 7.5 (2H,d), 7.6 (2H,d),7.7 (2H,s); ¹³C NMR (δ in ppm) – 26.1, 126.3,128.1, 130.4, 132.7,135.8,140.4; UV (λ_{max} in nm) - 269,395; Mass (M/Z): (189,272, 273 - [M+H] peak, 274 – [M+2H] peak).

2,5-bis(4-Hydroxybenzylidene)cyclopentanone

Yellow amorphous solid; yield-83%;mp: 192-194°C; IR (cm^{-1}) –3298,1668,1598, 1456,1386,988,839;¹H NMR (δ in ppm) – 3.02 (4H,s), 6.59(2H,d), 7.37(4H,d), 7.45(2H,s), 9.68 (2H,s); UV(λ_{max} in nm) - 258,393; Mass (M/Z): (186,254,293 - [M+H] peak).

2,5-bis(2-Furfurylidenebenzylidene) cyclopentanone

Orange needles;yield-79%;mp: 161-163°C; IR (cm^{-1})–1681,1620, 1601,1349; ¹H NMR (δ in ppm) – 3.02 (4H,s), 6.85 (2H,t), 7.65 (2H,d), 7.38 (2H,s), 8.16 (2H,d); UV(λ_{max} in nm) - 269,393.

Characterization

The IR spectra were obtained using a Thermo scientific Nicolet iS10 infrared spectrometer. The UV spectra were recorded using a Shimadzu UV-2450 spectrophotometer. The NMR spectra were recorded at 400 MHz using a Wormhole vnmrs-400 spectrometer. The Mass spectrometry was obtained via the ShimadzuQ2010 MS instrument.

Nonlinear Optical measurements

Powder SHG measurement

Kurtz and Perry have developed the powder SHG measurement which enables one to measure the SHG efficiency of materials using urea or potassium dihydrogen phosphate (KDP) as the standard (Smith and Galvin 1967; Kurtz and Perry 1968).

8 ns pulses of 1064 nm from Nd:YAG laser working at a repetition rate of 10Hz was used for SHG measurement. The microcrystalline powdered samples taken in glass capillary were smeared with laser pulses of energy ~ 3.1 mJ/pulse. A photomultiplier tube was used to detect the second harmonic wave of 532 nm produced from the sample and the resultant signal was fed into an oscilloscope. Urea 60 mV and KDP 27 mV were used as the standard reference materials.

Computational Studies

Gaussian 09 was used to perform the DFT optimization of the various molecules to study their energetics (Frisch et al. 2014), frequency profiles and NMR with the B3LYP/6-31G(d,p) level of theory^[9]. Further, these minimized conformations were used for docking studies with Auto-dock Vina. Autodock is the software tool for the estimation of the docked poses' binding affinity based on the genetic lamarkian algorithm. AutoDock-Vina is an upgrade to autodock developed by the Molecular Graphics Lab at the Scripps research institute that accurately predicts ligand receptor binding modes in a shorter time (Trott and Olson 2010). A 3.30Ghz Intel® Core™i5-4590 CPU system with 8GB RAM was used to carry out all the aforementioned calculations. Based on the biological activity to be evaluated for anti-inflammatory potential, the proteins for the desired mechanism are Porcine Thioredoxin Reductase and Bovine Lens Aldose Reductase whose crystal structures aren't available. Therefore, Human Aldose reductase (PDB 1US0) and Mammalian Thioredoxin reductase (PDB 1H6V) were chosen as these returned 96% and 89% similarity in a Basic Local Alignment Search Tool (BLAST) analysis. The PDB files of these proteins were obtained from the protein database (www.rcsb.org) and suitably cleaned for the additional heteroatoms and water molecules. 44 drugs with similar structural features as the parent class of cycloalkanes were obtained from the database to be docked onto the two proteins -TrxR and AldR. These were classified into four sets based on the substitution patterns on the parent cycloalkanes and docked into the active site of the aforementioned proteins (Katsori et al. 2011; Gromer et al. 2003). This helped arrive at correlative equations of significant linearity to enable the prediction of activity in corresponding families.

RESULTS AND DISCUSSION

ab Initio DFT computational studies

Three of the six analogues chosen returned transition states on DFT optimization their structures for least energy conformation using the B3LYP/6-31G(d,p) method of calculation. They were distorted in the direction of the imaginary frequency and optimized with tight convergence criteria, but failed to elicit a global minima. Hence, we report only the three optimized structures that attained a stable ground state.

2,5-Bis (2-furfurylidene)cyclopentanone

The optimised structure of 2,5-bis(2-Furfurylidenebenzylidene) cyclopentanone exhibited a C1 symmetry point group with the following computational results:

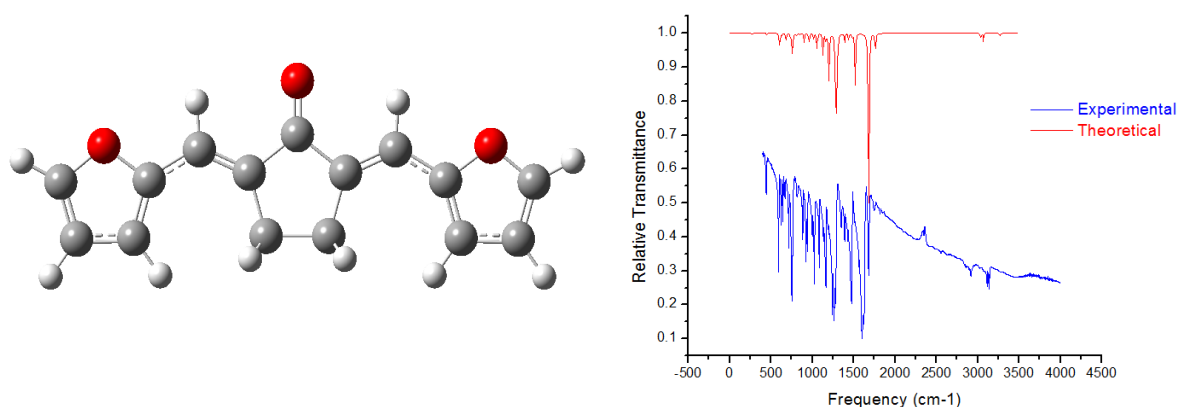


Figure1. Optimized DFT conformation structure and the predicted Vs experimental IR spectra of 2,5-Bis(2-furfurylidene)cyclopentanone.

The theoretical and experimentally obtained IR spectra were compared by plotting on Origin 7.0 and a maximum deviation of $\sim 35 \text{ cm}^{-1}$ was observed. The two plots were superimposed to evaluate for the extent of the peak to peak correlation as captured in Fig. 1. The frequencies in both the spectra with similar vibrational modes were identified for comparison as recorded in Table 1.

Table 1. Comparison of the experimental versus theoretical IR frequency modes of bis(2-Furfurylidene)cyclopentanone.

Experimental Frequency (cm^{-1})	Theoretical calculation (cm^{-1})		Assignment
	Unscaled	Scaled	
590.12	625.697	601.295	Cyclopentanone ring deformation
640.04	678.333	651.878	Cyclopentanone ring deformation
713.84	734.312	705.674	-CH ₂ - rocking
923.88	962.926	925.372	Alkene H oop bending
1022.06	1055.26	1014.11	
1083.18	1130.3	1086.218	Furan C-H deformation
1135.24	1186.44	1140.169	
1162.15	1201.49	1154.632	
1243.40	1307.97	1256.959	-CH ₂ - wagging
1349.28	1387.41	1333.301	Alkene H in plane bending
1427.13	1486.03	1428.075	-CH ₂ - scissoring
1473.53	1518.64	1459.413	Furan C=C stretching
1601.26	1670.64	1605.485	Alkene C=C stretch symmetric
1621.21	1678.63	1613.163	Alkene C=C stretch asymmetric
1681.09	1765.87	1697.001	C=O stretching
2915.87	3069.53	2949.818	-CH ₂ - stretch
3114.28	3265.62	3138.261	Furan C-H stretch symmetric
3134.20	3297.24	3168.648	Furan C-H stretch asymmetric

As recorded in the Table 1 and Fig. 1, we see that the correlation is nearly unity obtained using the 6-31G(d,p) that proves to be a significantly appropriate basis set of choice for this molecule given the matching peaks observed across most of the modes. The C-H furan stretching exhibits the maximum deviation of 34 cm^{-1} while the characteristic carbonyl stretch shows good agreement with the experimental value, showing a deviation of 16 cm^{-1} . The other characteristic peaks like the scissoring, bending and alkene stretch show very less deviation, demonstrating the reliability of the chosen 6-31G(d,p) basis set that comes close to accurately describing the system. In general, the observed deviation at smaller frequencies is lesser than the higher frequencies. Similarly, the experimental and theoretical bond lengths and bond angles were compared for a good correlation in the structural prediction with the chosen basis set.

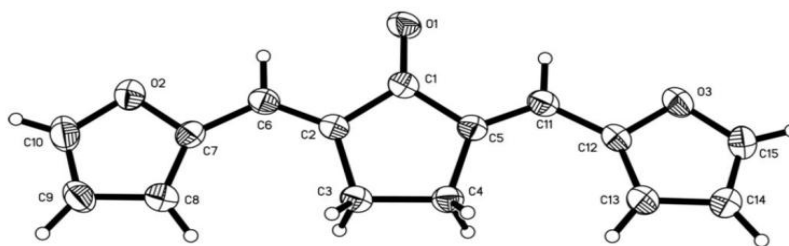


Figure 2. ORTEP diagram of 2,5-bis(2-Furfurylidene)cyclopentanone with the atom-numbering scheme. Displacement ellipsoids are drawn at the 30% probability level and H atoms are shown as small spheres of arbitrary radius.

On comparing the experimental values reported for the structure (Ma and Zheng 2009), with the theoretical values obtained from the simulations, a good correlation is observed.

Table 2. Comparison of the experimental versus theoretical structural parameters of the synthesized molecule –bis(2-Furfurylidene)cyclopentanone.

Coordinates	Expt.(Θ°)	Theoretical(Θ°)	Coordinates	Expt.(Θ°)	Theoretical(Θ°)
C10-O2-C7	106.5(2)	107.5	C8—C7—C6	136.4(3)	135.6
C15-O3-C12	106.8(2)	107.5	O2—C7—C6	115.1(2)	115.7
O1-C1-C2	125.6(3)	126.3	C7—C8—C9	107.6(3)	107.0
O1-C1-C5	125.8(2)	126.3	C7—C8—H8	126.2	126.2
C2-C1-C5	108.6(2)	107.4	C9—C8—H8	126.2	126.9
C6-C2-C1	121.2(2)	120.5	C10-C9-C8	106.0(3)	106.1
C6-C2-C3	129.1(2)	129.3	C10-C9-H9	127.0	126.5
C1-C2-C3	109.7(2)	110.2	C8-C9-H9	127.0	127.4
C2-C3-C4	106.2(2)	106.1	C9-C10-O2	111.4(3)	110.7
C2-C3-H3A	110.5	111.2	C9-C10-H10	124.3	133.3
C4-C3-H3A	110.5	111.2	O2-C10-H10	124.3	116.0
C2-C3-H3B	110.5	111.2	C5-C11-C12	128.1(2)	127.4
C4-C3-H3B	110.5	11.2	C5-C11-H11	115.9	116.6
H3A-C3-H3B	108.7	106.2	C12-C11-H11	115.9	116.1
C5-C4-C3	106.2(2)	106.1	C13-C12-O3	108.6	108.7
C5-C4-H4A	110.5	111.2	C13-C12-C11	135.6(3)	135.6
C3-C4-H4A	110.5	111.2	O3-C12-C11	115.7(2)	115.7
C5-C4-H4B	110.5	111.2	C12-C13-C14	107.5(3)	107.0
C3-C4-H4B	110.5	111.2	C12-C13-H13	126.2	126.2
H4A-C4-H4B	108.7	106.2	C14-C13-H13	126.2	126.9
C11-C5-C1	121.2(2)	120.5	C15-C14-C13	106.4(3)	106.1
C11-C5-C4	129.4(2)	129.3	C15-C14-H14	126.8	126.5
C1-C5-C4	109.3(2)	110.2	C13-C14-H14	126.8	127.4
C2-C6-C7	128.6(2)	127.4	C14-C15-O3	110.8(3)	110.7
C2-C6-H6	115.7	116.6	C14-C15-H15	124.6	133.3
C7-C6-H6	115.7	116.1	O3-C15-H15	124.6	116.0
C8-C7-O2	108.2(4)	108.7			
Coordinates	Expt.(A°)	Theoretical(A°)	Coordinates	Expt.(A°)	Theoretical(A°)
O1-C1	1.237(3)	1.228	C6-C7	1.425(3)	1.432
O2-C10	1.350(3)	1.354	C6-H6	0.9300	1.088
O2-C7	1.377(3)	1.379	C7-C8	1.347(3)	1.381
O3-C15	1.356(3)	1.354	C8-C9	1.412(2)	1.423
O3-C12	1.375(3)	1.379	C8-H8	0.9300	1.079
C1-C2	1.463(3)	1.485	C9-C10	1.326(4)	1.366
C1-C5	1.471(3)	1.485	C9-H9	0.9300	1.080
C2-C6	1.335(3)	1.353	C10-H10	0.9300	1.079
C2-C3	1.490(3)	1.507	C11-C12	1.426(4)	1.432
C3-C4	1.552(3)	1.560	C11- H11	0.9300	1.088
C3-H3A	0.9700	1.097	C12-C13	1.341(3)	1.381
C3-H3B	0.9700	1.097	C13-C14	1.415(4)	1.423
C4-C5	1.493(3)	1.507	C13-H13	0.9300	1.079
C4-H4A	0.9700	1.097	C14-C15	1.324(3)	1.366
C4-H4B	0.9700	1.097	C14-H14	0.9300	1.079
C5-C11	1.335(3)	1.353	C15-H15	0.9300	1.079

There is a slight discrepancy observed in the furan ring that is shrunk inward as indicated by the C8-C9 and C7-C8 bond lengths which could be attributed to the extended conjugation that can exist between the double bonds and the furan ring, causing the bonds to shrink and possess enhanced 's' character. This is further supported by the fact that the C-H bonds in the crystal are shorter than the theoretical model due to increased 's' character provided by conjugation. Thus, it is seen that long range conjugation is not completely incorporated into the chosen computational model. Perhaps a better model will be attained by using basis sets that incorporate the diffuse functional for the hydrogen. On observing the bond angles, the theoretical model is close to the actual crystal structure barring the angles involving the C10 and C15 hydrogens which appears more towards the oxygen than that of the crystal structure. This could be due to the interaction of the hydrogen with the oxygen. In the crystal structure, there are neighboring oxygen atoms in the adjoining lattice available for interactions unlike the theoretical model treated as a unique isolated system in vacuum. Hence the hydrogen is more displaced from the oxygen in comparison to the theoretical model as indicated by the O2-C10-H2 and O3-C15-H15 bond angles. This trend is observed with all the hydrogens in the theoretical model, which are more displaced in the direction of the oxygen atom.

(2S,2E)-2,5-Bis (thiophenyl-2-methylene)cyclopentanone

The optimised structure of (2S,2E)-2,5-Bis (thiophenyl-2-methylene) cyclopentanone demonstrated a C1 point group of symmetry with the following computational results:

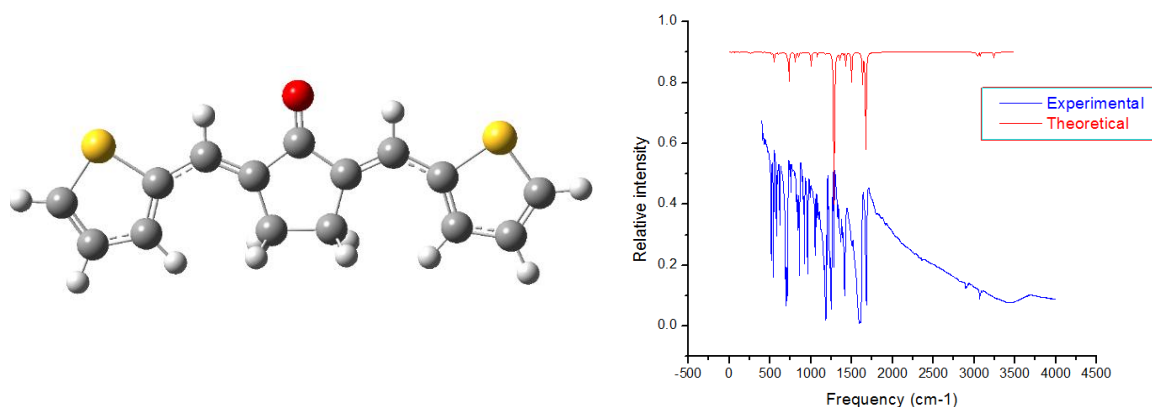


Figure 3. The structure of the optimized DFT conformation and the predicted Vs experimental IR spectra of (2S,2E)-2,5-Bis(thiophenyl-2-methylene)cyclopentanone molecule.

Table 3. Comparison of the experimental versus theoretical IR frequency modes of the (2S,2E)-2,5-Bis(thiophenyl-2-methylene)cyclopentanone molecule.

Expt. Freq. (cm ⁻¹)	Theoretical (cm ⁻¹)		Assignment
	Unscaled	Scaled	
592.89	627.733	603.2514	Cyclopentanone ring deformation
692.67	728.388	699.9809	Thiophene C-H oop bending
706.07	737.034	708.2897	-CH ₂ - rocking
826.15	848.567	815.4729	Thiophene ring C-H deformation
842.92	861.396	827.8016	Thiophene C-H oop bending
859.8	883.918	849.4452	Thiophene C-H oop bending
959.95	999.719	960.73	Cyclopentanone ring deformation
1052.8	1083	1040.763	Thiophene ring C-H deformation
1067.91	1124.45	1080.596	Thiophene ring C-H deformation
1228.96	1282.09	1232.088	Cyclopentanone ring deformation
1250.23	1305	1254.105	-CH ₂ - wagging
1280.5	1352.94	1300.175	-CH ₂ - wagging
1413.1	1499.67	1441.183	Thiophene C=C stretch
1593.6	1668.23	1603.169	Alkene C=C stretch
1680.83	1711.2	1644.463	C=O stretch

The theoretical and experimentally obtained IR spectra were compared by plotting on Origin 7.0 and a maximum deviation of $\sim 36\text{ cm}^{-1}$ was observed. The two plots were made to overlap to observe whether there was any peak to peak correlation. The frequencies in both the spectra with similar vibrational modes were identified and assigned using IR frequency correlation tables. On observing the table and the graph we see that the correlation obtained using the 6-31G(d,p) is a very good one with almost peak to peak matching. The C=O stretch shows the maximum deviation of 36 cm^{-1} which is a decent agreement with the experimental value. The other characteristic peaks like the scissoring, bending and alkene stretch show less deviation, showing that the basis set used 6-31G(d,p) comes close to accurately describing the system. The table consists of only those frequencies which were found in both the experimental and theoretical spectra as there are some bands that were predicted but not observed.

2,5-Bis(4-hydroxybenzylidene) cyclopentanone

The optimised structure of 2,5-bis(4-hydroxybenzylidene) cyclopentanone showed symmetry characteristic of the C₁ point group with the following computational results:

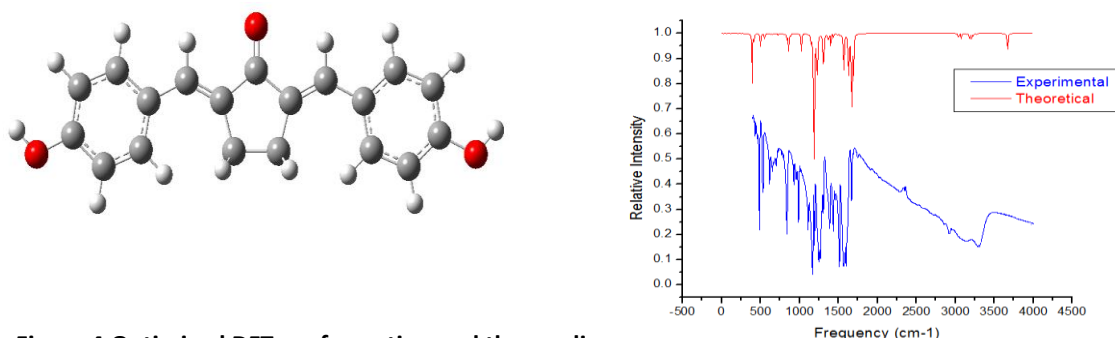


Figure 4. Optimized DFT conformation and the predicted IR spectrum of 2,5-bis(4-hydroxybenzylidene)cyclopentanone.

The theoretical and experimentally obtained IR spectra were compared by plotting on Origin 7.0 and a maximum deviation of $\sim 55\text{ cm}^{-1}$ was observed. The two plots were made to overlap to observe whether there was any peak to peak correlation. The frequencies in both the spectra with similar vibrational modes were identified and assigned using IR frequency correlation tables. The theoretical and experimental spectra along with the associated assignments are as follows:

Table 4. Comparison of the experimental versus theoretical IR frequency modes of the 2,5-Bis(4-hydroxybenzylidene)cyclopentanone molecule.

Expt. Freq. (cm ⁻¹)	Theoretical calculation (cm ⁻¹)		Assignment
	Unscaled	Scaled	
838.7	862.891	829.2383	Aromatic CH out of plane bending
987.59	971.665	933.7701	Ring breathing
1108.55	1150.54	1105.669	Deformation of aromatic C-H
1188.99	1225	1177.225	O-H bend
1247.81	1317.61	1266.223	Asymmetric -CH ₂ - wagging
1266	1359.08	1306.076	Symmetric -CH ₂ - wagging
1307.34	1308.71	1257.67	C-O-H bending
1385.96	1443.78	1387.473	Alkene C-H in plane bending
1450.07	1522	1462.642	-CH ₂ - scissoring
1566.29	1630.7	1567.103	Asymmetric Aromatic C=C stretch
1598.15	1666.36	1601.372	Symmetric Aromatic C=C stretch
1668.01	1726.06	1658.744	C=O stretch
3297.83	3666.54	3523.545	O-H stretch

As recorded in the table 4 and the graph, we see that the correlation obtained using the 6-31G(d,p) is a very good one with almost peak to peak matching. The ring breathing vibration shows the maximum deviation of 54cm^{-1} which is a decent agreement with the experimental value. The other characteristic peaks like the carbonyl stretch, scissoring, bending and alkene stretch show less deviation, showing that the basis set used, 6-31G(d,p), comes close to accurately describing the system. There seems to be one anomaly observed with regards to the O-H peak alluding to the presence of water in the system despite keeping it dry. However, this exhibited broad peak corresponds to the intermolecular hydrogen bonding in the system via the hydroxyl groups. The table consists of only those frequencies which were found in both the experimental and theoretical spectra as there are some bands that were predicted but not observed.

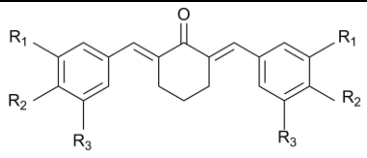
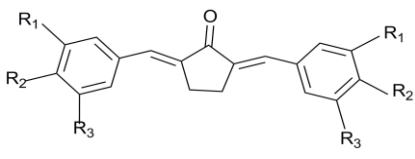
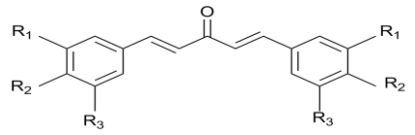
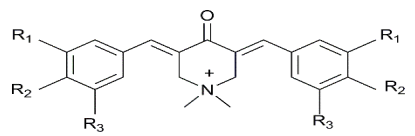
Non Linear Optics

The second harmonic generation of the synthesized cyclopentanone analogues was measured, with urea (0.13×10^{-30} esu) used as reference (Adant, Dupuis, and Bredas 1995). The data associated with the analogues is recorded in Table 5. The presence of chlorine in the meta position doesn't contribute to the increase of electron density on the carbonyl oxygen as opposed to the presence of chlorine in the ortho group, due to its weak electron pumping nature. This is the reason for the mild SHG property shown by the 2-chloro analogue. Further, the furyl and the thienyl analogues show zero SHG property as the heterocyclic rings are not good electron donors. The interesting observation comes in the case of the hydroxyl analogues which contain very good electron donors.

Table 5. Comparison of the NLO activity as demonstrated with respect to the Urea and KDP standards.

Cyclopentanone analog	Comparison (Ref: Urea)
2,5-Bis(2-chlorobenzylidene)cyclopentanone	0.4124
2,5-Bis(3-chlorobenzylidene)cyclopentanone	0
2,5-Bis(2-furfurylidene)cyclopentanone	0
2,5-Bis((2-thienyl)methylidene)cyclopentanone	0
2,5-Bis(2-hydroxybenzylidene)cyclopentanone	0
2,5-Bis(4-hydroxybenzylidene)cyclopentanone	0.2167

Table 6. The relationship between the activity and the binding affinity with respect to each of the various classes across both the pathways for anti-inflammatory activity prediction.

Parent class	S.No	Correlation Equation	r^2 (n)
	TrxR Set 1 AldR Set 1	$y = 10.436x + 107.69$ $y = 13.802x + 173.98$	0.72 (5) 0.78 (6)
	TrxR Set 2 AldR Set 2	$y = 20.092x + 192.59$ $y = 11.339x + 141.34$	0.84 (5) 0.74 (6)
	TrxR Set 3 AldR Set 3	$y = 7.0511x + 61.004$ $y = 23.539x + 275.26$	0.86 (5) 0.62 (5)
	TrxR Set 4 AldR Set 4	$y = 117.68x + 989.7$ $y = 8.9553x + 116.47$	0.83 (6) 0.76 (6)

As noted in the above data set, the importance of the position of the electron donors is highlighted. As the hydroxyl is present in the ortho position of the ring, it has close proximity to the ketone group and can exhibit hydrogen bonding. This reduces the electron density on the carbonyl oxygen and hence shows zero SHG property. On the other hand, the para position is far away for any interactions of the oxygen and hydrogen to exist. Hence it shows mild SHG property.

Molecular Docking Studies

44 derivatives across two databases undergoing the TrxR (*thioredoxin reductase*) pathway and the AldR (*Aldose reductase*) pathway were obtained and classified into four sets to be docked against both receptors. The correlation equation for cyclopentanone analogues was obtained from the plot of the known IC₅₀ values against binding affinities for the ligands obtained from docking studies. These values were then input into the correlation equations for the corresponding synthesized ligands whose activity (pIC₅₀) was predicted as tabulated (Table 6). We observe in table 6 that our synthesized analogs in general demonstrate promising activity better through the TrxR pathways vis-à-vis the AldR pathway. We note the significant relationship ~ 8 on an average across all the data sets confirming this route to predict the activity of the analogs from their estimated binding affinity. Thus, using these formulae, we calculated the anti-inflammatory potential of the six analogs synthesized as tabulated (Table 7). There is clearly one specific derivative of interest from the recorded data in the 2,5-bis(3-Chlorobenzylidene)cyclopentanone molecule that exhibits a significant calculated pIC₅₀ of ~ 7.8 μ M in the *thioredoxin reductase* pathway comparable to the standard drugs prescribed. This could accordingly be evaluated *in vitro* for the anti-inflammatory activity and further modeled as a potential lead. In this regard, we undertook the qualitative SAR of these compounds with the aforementioned data set.

Table 7. The predicted activity of the six analogs for the two pathways as determined from the correlation equations obtained by docking studies.

Synthesized Analog	BA_TrxR (Kcal/mol)	pIC ₅₀ _TrxR (μ M)	BA_AldR (Kcal/mol)	pIC ₅₀ _AldR (μ M)
2,5-bis(2-Chlorobenzylidene)cyclopentanone	-8.4	23.82	-9.1	38.16
2,5-bis(3-Chlorobenzylidene)cyclopentanone	-9.2	7.74	-9.5	33.62
2,5-bis(2-Hydroxybenzylidene)cyclopentanone	-8.1	29.85	-9.9	29.08
2,5-bis(2-Furfurylidene)cyclopentanone	-7.1	48.76	-8.6	43.83
2,5-bis((2-Thienyl)methylidene)cyclopentanone	-6.8	55.97	-7.4	57.43

Structure Activity Relationship

TrxR (thioredoxin reductase) pathway

The vital role of a hydroxyl group in the inhibition of TrxR. While the presence of two hydroxyls in the R1 and R2 positions increase the inhibitory effect of the molecule, the replacement of a hydroxyl with a methoxyl drastically reduces the inhibitory potency, suggesting the importance of the hydrogen in interacting with the binding site and its role in inhibition. The replacement of the electron donating methoxyl group with the deactivating bromine atom only slightly affects inhibition, supported by the marginal increase in the inhibition concentration. The presence of a methoxyl drastically improves the binding affinity in the cyclopentanone analogue. The replacement of a methoxyl with bromine affects the binding energy by almost 1 Kcal. The presence of the bulky tertiary-butyl group affects its binding affinity, reducing it by almost 2.0 Kcal. The presence of a single hydroxyl has better binding affinity and inhibition than a di-hydroxy substitution. Lack of rigidity owing to absence of the cyclopentanone or cyclohexanone core leads to lower average binding affinity although here the other factors need to be considered in addition. A net positive charge lowers the binding affinity that directly affecting the inhibition concentration. The replacements of hydrogen with methoxy groups at R1 and R3 drastically increases the inhibition and binding energy owing to either the electron pumping nature of the methoxyl groups that stabilizes the positive charge on nitrogen.

AldR (Aldose reductase) pathway

The presence of the bulky tert-butyl group decreases the binding energy by almost a unit highlighting the steric factors responsible for binding while the presence of methoxyl groups enhances the inhibitory effect, highlighting the importance of electron pumping groups at R1 and R3. The addition of a hydroxyl at R1 increases the binding affinity while the replacement of a methoxyl by a halide group doesn't affect the binding affinity to a large effect.

The presence of the electron donating hydroxyl group at R1 is vital in improving the binding affinity enhancing by almost 2.5Kcal. Ring size too has a major influence on the binding characteristics of these ligands. The presence of a di-hydroxy substitution vastly enhances while the replacement of the tert-butyl groups by methoxyl groups only marginally increases the binding affinity. The replacement of the hydroxyl with a methoxyl largely reduces the binding affinity and increases the activity suggesting the importance of hydrogen bonding in the inhibition mechanism and the interaction of the ligand with the binding site. Substitutions in the R1 and R3 positions of ligand 20 with the tertiary butyl group only marginally improve the binding affinity, suggesting that the R2 position plays an important role in binding and that substitutions in the R1 and R3 positions don't affect the binding affinity to a large extent.

The corresponding best docked pose for the two molecules with the potential for maximal anti-inflammatory activity using both the proposed mechanisms is captured from the molecular docking studies using PyMol visualization software. These interactions are accordingly presented in Fig. 5 with the site of interactions highlighted.

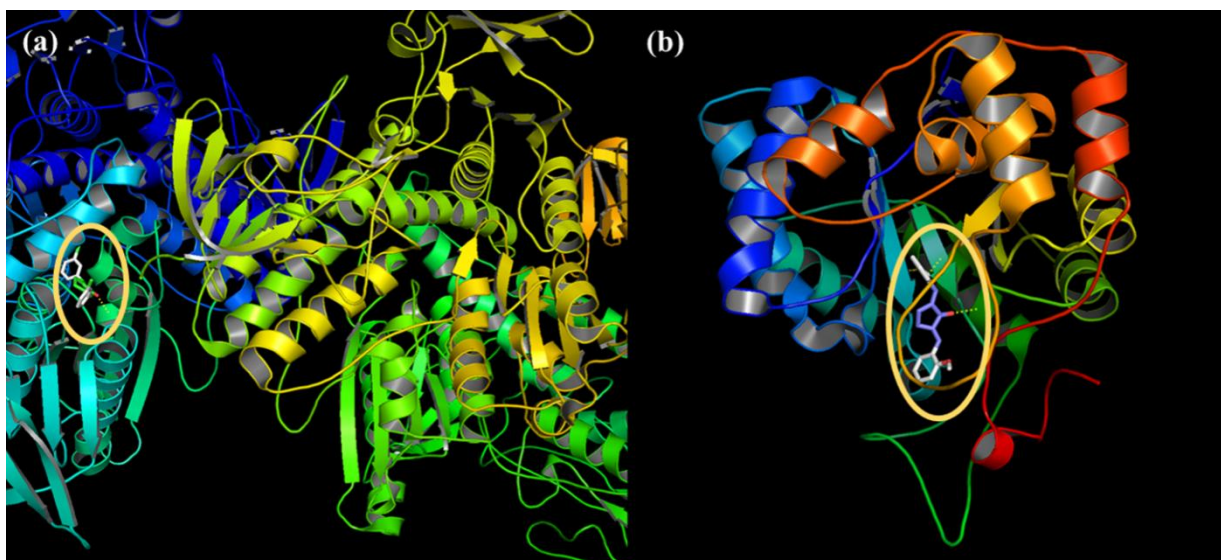


Figure 5. The best docked pose of the two ligands with best binding affinity as determined by the molecular docking studies: (a) 2,5-Bis(3-chlorobenzylidene) cyclopentanone with Mammalian Thioredoxin reductase (PDB 1H6V), and (b) 2,5-Bis(2-hydroxybenzylidene) cyclopentanone in the Human Aldose reductase (PDB 1US0).

CONCLUSION

Six dibenzylidenecyclopentanone analogues of curcumin were synthesized and confirmed for their structures by extensive characterization with IR, UV, NMR and MS. Their Non Linear Optical properties were determined experimentally and the findings observed. The *ab initio* DFT optimization of the molecules was undertaken with the B3LYP/6-31G (d,p) basis set to derive least energy conformers with appreciable spectral and structural correlation against the experimental findings for 3 of the analogs. The minor deviations and divergence for the other three analogs propose the search for a further immaculate basis set. *In silico* studies helped predict the activity using docking scores of cyclopentanone derivatives against Mammalian Thioredoxin reductase to be further confirmed upon testing with an MTT assay. One molecule of interest that could be explored as a potential lead was 2,5-Bis(3-chlorobenzylidene)cyclopentanone. Further to enhance their efficacy, we determined the qualitative structure activity relationship for the modeling of these derivatives for the anti-inflammatory activity against the two pathways. We demonstrated the importance of hydroxyl group and electron pumping groups at R1 and R3 in the *thioredoxin reductase* pathway, while the importance of electron pumping groups and ring size with R2 as the key position in the *Aldose reductase* pathway.

ACKNOWLEDGMENTS

We are grateful to Bhagawan Sri Sathya Sai Baba, the founder chancellor, SSSIHL for his constant inspiration to serve the society. We are indebted to the administration of SSSIHL for their support for the work undertaken.

REFERENCES

- Adant, C., M. Dupuis and J. L. Bredas (1995).** "Ab Initio Study of the Nonlinear Optical Properties of Urea: Electron Correlation and Dispersion Effects." *International Journal of Quantum Chemistry* 56 (S29). Wiley Online Library: 497–507.
- Anand Preetha, Ajaikumar, B. Kunnumakkara, Robert A. Newman and Bharat B Aggarwal (2007).** "Bioavailability of Curcumin: Problems and Promises." *Molecular Pharmaceutics* 4 (6). ACS Publications: 807–18.
- Benassi Rois, Erika Ferrari, Sandra Lazzari, Ferdinando Spagnolo and Monica Saladini (2008).** "Theoretical Study on Curcumin: A Comparison of Calculated Spectroscopic Properties with NMR, UV–Vis and IR Experimental Data." *Journal of Molecular Structure* 892 (1–3). Elsevier: 168–76.
- Bukhari Syed Nasir Abbas, Ibrahim Bin Jantan, Malina Jasamai, Waqas Ahmad and Muhammad Wahab Bin Amjad (2013).** "Synthesis and Biological Evaluation of Curcumin Analogues." *J. Med. Sci* 13 (7): 501–13.
- Chen Bohong, Zhibo Zhu, Min Chen, Wenqi Dong and Zhen Li (2014).** "Three-Dimensional Quantitative Structure–Activity Relationship Study on Antioxidant Capacity of Curcumin Analogues." *Journal of Molecular Structure* 1061. Elsevier: 134–39.
- Corn Robert M. and Daniel A. Higgins (1994).** "Optical Second Harmonic Generation as a Probe of Surface Chemistry." *Chemical Reviews* 94 (1). ACS Publications: 107–25.
- Dinkova-Kostova, Albena, T. and Paul Talalay (2008).** "Direct and Indirect Antioxidant Properties of Inducers of Cytoprotective Proteins." *Molecular Nutrition & Food Research* 52 (S1). Wiley Online Library: S128–S138.
- Du Zhi-Yun, Ya-Dan Bao, Zhong Liu, Wei Qiao, Lin Ma, Zhi-Shu Huang, Lian-Quan Gu and Albert S. .C Chan (2006).** "Curcumin Analogs as Potent Aldose Reductase Inhibitors." *Archiv Der Pharmazie: An International Journal Pharmaceutical and Medicinal Chemistry* 339 (3). Wiley Online Library: 123–28.
- Frisch, M. J., G. W. Trucks, H. B. Schlegel, G. E. Scuseria, M. A. Robb, J. R. Cheeseman, G. Scalmani, et al. (2014).** "Official Gaussian 09 Literature Citation."
- Gromer Stephan, Linda Johansson, Holger Bauer, L. David Arcsott, Susanne Rauch, David P. Ballou, Charles, H. Williams, R. Heiner Schirmer and Elias, S. J. Arnér (2003).** "Active Sites of Thioredoxin Reductases: Why Selenoproteins?" *Proceedings of the National Academy of Sciences* 100 (22). National Acad Sciences: 12618–23.
- Katsori, A.M., M. Chatzopoulou, K. Dimas, C. Kontogiorgis, A. Patsilinos, T. Trangas and D. Hadjipavlou-Litina (2011).** "Curcumin Analogues as Possible Anti-Proliferative & Anti-Inflammatory Agents." *European Journal of Medicinal Chemistry* 46 (7). Elsevier: 2722–35.
- Kurtz, S. K. and T. T. Perry (1968).** "A Powder Technique for the Evaluation of Nonlinear Optical Materials." *Journal of Applied Physics* 39 (8). AIP: 3798–3813.
- Leow, Pay-Chin, Priti Bahety, Choon Pei Boon, Chong Yew Lee, Kheng Lin Tan, Tianming Yang and Pui-Lai Rachel Ee (2014).** "Functionalized Curcumin Analogs as Potent Modulators of the Wnt/ β -Catenin Signaling Pathway." *European Journal of Medicinal Chemistry* 71. Elsevier: 67–80.
- Liang Guang, Xiaokun Li, Li Chen, Shulin Yang, Xudong Wu, Elaine Studer, Emily Gurley, et al. (2008).** "Synthesis and Anti-Inflammatory Activities of Mono-Carbonyl Analogues of Curcumin." *Bioorganic & Medicinal Chemistry Letters* 18 (4). Elsevier: 1525–29.
- Liang Guang, Lili Shao, Yi Wang, Chengguang Zhao, Yanhui Chu, Jian Xiao, Yu Zhao, Xiaokun Li and Shulin Yang (2009).** "Exploration and Synthesis of Curcumin Analogues with Improved Structural Stability Both in Vitro and in Vivo as Cytotoxic Agents." *Bioorganic & Medicinal Chemistry* 17 (6). Elsevier: 2623–31.
- Liang Guang, Shulin Yang, Huiping Zhou, Lili Shao, Kexin Huang, Jian Xiao, Zhifeng Huang and Xiaokun Li (2009).** "Synthesis, Crystal Structure and Anti-Inflammatory Properties of Curcumin Analogues." *European Journal of Medicinal Chemistry* 44 (2). Elsevier: 915–19.
- Liu Zhong, Zhi-Yun Du, Zhi-Shu Huang, Kin-Sing Lee and Lian-Quan Gu (2008).** "Inhibition of Thioredoxin Reductase by Curcumin Analogs." *Bioscience, Biotechnology, and Biochemistry* 72 (8). Japan Society for Bioscience, Biotechnology, and Agrochemistry: 2214–18.

- Ma, S.Y. and Z.B. Zheng (2009). "(2E, 5E)-2, 5-Difurfurylidene-cyclopentanone." *Acta Crystallographica Section E: Structure Reports Online* 65 (12). International Union of Crystallography: o3084--o3084.
- Saleem, H., Akhil, R. Krishnan, Y. Erdogdu, S. Subashchandrabose, V. Thanikachalam and G. Manikandan (2011). "Density Functional Theory Studies on 2, 5-Bis (4-Hydroxy-3-Methoxybenzylidene) Cyclopentanone." *Journal of Molecular Structure* 999 (1–3). Elsevier: 2–9.
- Shang, Ya-Jing, Xiao-Ling Jin, Xian-Ling Shang, Jiang-Jiang Tang, Guo-Yun Liu, Fang Dai, Yi-Ping Qian, Gui-Juan Fan, Qiang Liu and Bo Zhou (2010). "Antioxidant Capacity of Curcumin-Directed Analogues: Structure--Activity Relationship and Influence of Microenvironment." *Food Chemistry* 119 (4). Elsevier: 1435–42.
- Shen Liang and Hong-Fang Ji (2007). "Theoretical Study on Physicochemical Properties of Curcumin." *Spectrochimica Acta Part A: Molecular and Biomolecular Spectroscopy* 67 (3–4). Elsevier: 619–23.
- Shen Liang, Hong-Fang Ji and Hong-Yu Zhang (2005). "A TD-DFT Study on Triplet Excited-State Properties of Curcumin and Its Implications in Elucidating the Photosensitizing Mechanisms of the Pigment." *Chemical Physics Letters* 409 (4–6). Elsevier: 300–303.
- Smith, R. and M. Galvin (1967). "Operation of the Continuously Pumped, Repetitive Q-Switched YAG: Nd Laser." *IEEE Journal of Quantum Electronics* 3 (10). IEEE: 406–14.
- Trott Oleg and Arthur, J. Olson (2010). "AutoDock Vina: Improving the Speed and Accuracy of Docking with a New Scoring Function, Efficient Optimization, and Multithreading." *Journal of Computational Chemistry* 31 (2). Wiley Online Library: 455–61.
- Wang Yi, Congcong Yu, Yong Pan, Xuyi Yang, Yi Huang, Zhiguo Feng, Xiaokun Li, Shulin Yang and Guang Liang (2012). "A Novel Synthetic Mono-Carbonyl Analogue of Curcumin, A13, Exhibits Anti-Inflammatory Effects in Vivo by Inhibition of Inflammatory Mediators." *Inflammation* 35 (2). Springer: 594–604.
- Zhao Chengguang, Yuepiao Cai, Xuzhi He, Jianling Li, Li Zhang, Jianzhang Wu, Yunjie Zhao, et al. (2010). "Synthesis and Anti-Inflammatory Evaluation of Novel Mono-Carbonyl Analogues of Curcumin in LPS-Stimulated RAW 264.7 Macrophages." *European Journal of Medicinal Chemistry* 45 (12). Elsevier: 5773–80.

Corresponding author: Dr. B. Siva Kumar, Assistant Head, Department of Chemistry, Sri Sathya Sai Institute of Higher Learning, Vidyagiri Road, Puttaparthi, (A.P), India- 515134

Email: bsivakumar@sssihl.edu.in

Ph: +91-9440547264